Electronic Supplementary Information

Self-powered HgTe quantum dots/PBDB-T:Y6 bipolar broadband photodetector for logic gates

Wenxin Zeng,[a] Zaihua Duan,*[a] Yichen Bu,[a] Haichao Yu,[b] Changhong Wang,[b] Xing Tang,[a] Jingwen Yang,[a] Zhen Yuan,[a] Yadong Jiang[a] and Huiling Tai*[a]

[a]*State Key Laboratory of Electronic Thin Films and Integrated Devices, School of Optoelectronic Science and Engineering, University of Electronic Science and Technology of China (UESTC), Chengdu 611731, China*

E-mail: zaihuaduan@uestc.edu.cn, taitai1980@uestc.edu.cn

[b]*49th Research Institute of China Electronics Technology Group Corporation, Harbin 150028, China*

Experimental section

Materials

Mercury chloride ($HgCl_2$, Sigma-Aldrich, 99%), Tellurium (Te, Aladdin, 99.99%), Oleylamine (OLA, Aladdin, 80-90%), Tri-n-octylphosphine (TOP, Aladdin, 90%), Methanol (MeOH, Aladdin, 99%), Toluene (CHRON CHEMICALS, 99.5%), Octane (OCT, Aladdin, >99%), Isopropanol (IPA, Aladdin, >99.7%), 1,2-ethanedithiol (EDT, Aladdin, 99.5%), 1-Dodecanethiol (DDT, Aladdin, 98%), Tetrachloroethylene (TCE, Aladdin, 99%), PBDB-T (Solarmer Materials Inc, 99%), Y6 (Solarmer Materials Inc, 99%), 1,2-dichlorobenzene (o-DCB, Sigma-Aldrich, >99%), MoO_3 (ZhongNuo Advanced Material (Beijing) Technology Co. Ltd., 99%), Ag (ZhongNuo Advanced Material (Beijing) Technology Co. Ltd., 99%), ZnO (ZhongNuo Advanced Material (Beijing) Technology Co. Ltd., 99%).

Synthesis of the HgTe QDs

Pre-purified of OLA: The purification of OLA was carried out at 120 °C under vacuum for 3 h, and finally stored it in a glovebox.

Stock solution of Te precursor TOPTe (1 mol/L): 0.3828 g (3 mmol) Te was added into a 20 mL three-neck flask containing 3 mL of TOP. The three necked flask was heated to 120 °C and degassed for 30 min. Then, the atmosphere was switched to nitrogen, and the temperature was increased to 200 °C. The mixture was stirred continuously for 3 h to obtain a clear orange solution. The mixture was cooled to room temperature to obtain a clear yellow 1 M TOPTe precursor solution, and stored in a glovebox.

Synthesis of HgTe seeds: In a 100 mL three-neck flask, 246 mg (0.9 mmol) of $HgCl_2$ was added to 5 mL of pre-purified OLA and degassed at 100 °C for 1 h. After degassing, the mixture

was stirred continuously at 100 °C for 30 min to ensure complete dissolution of $HgCl_2$. Then, the atmosphere was switched to nitrogen, the temperature of the mixture was reduced to 35 °C, 0.6 mL of 1M TOPTe precursor solution was rapidly injected into the reaction mixture, and the reaction lasted for 10 min. The solution changed from white to black, suggesting the formation of HgTe seeds. Next, 1 mL of HgTe seeds solution was taken out, and the reaction was quenched by adding a mixed solution of 0.4 mL of DDT and 0.2 mL of TOP in 4 mL of TCE. After quenching, the solution was precipitated with an equal volume of MeOH and centrifuged at 7000 rpm for 3 min, the precipitate was resuspended in 5 mL of toluene. The solution was precipitated a second time with an equal volume of MeOH, the precipitate was dried and then resuspended in octane.

Oriented crystallization of HgTe QDs: 5 mL of pre-purified OLA was added into a 100 mL three-neck flask, and degassed at 100 °C for 1 h. Then, the atmosphere was switched to nitrogen, and the temperature was adjusted to 60 °C. 1 mL HgTe seeds were rapidly injected into the OLA, and the reaction lasted for 3 min. The reaction was quenched by adding a mixed solution of 0.4 mL of DDT and 0.2 mL of TOP in 4 mL of TCE. The temperature of the reactants is reduced by ice bath. After quenching, the solution was precipitated with an equal volume of MeOH and centrifuged at 7000 rpm for 3 min, the precipitate was resuspended in 5 mL of toluene. The solution was precipitated a second time with an equal volume of MeOH, the precipitate was dried and then resuspended in octane.

Materials characterizations

The X-ray diffraction (XRD) was conducted by Rigaku SmartLab 9 kW diffractometer. The transmission electron microscopy (TEM) samples were prepared by putting 1 drop of the

solution (100 μg/mL) onto a carbon-coated Cu grid. Cross-sectional samples (t = 100 nm) for the TEM measurement were obtained using focused-ion beam (FIB) system (Helios UC). The morphology, crystalline structure of HgTe QDs, cross-sectional TEM images of the BPD and EDS element mappings were performed by a JEOL 2100 Plus TEM. Optical absorption spectra of the PBDB-T:Y6 and HgTe QDs solutions, and the absorption spectrum of PBDB-T:Y6 and HgTe QDs films were collected using a Shimadzu UV-3600 plus spectrophotometer. The scanning electron microscope (SEM) images were collected using ZEISS GeminiSEM 300 scanning electron microscope. The ultraviolet photoelectron spectroscopy (UPS) measurements were performed on an electron spectrometer using the monochromatic HeI radiation 21.22 eV of Thermo Scientific-ESCALAB Xi+ in ultra-high vacuum conditions at 10 V bias.

Device fabrication and measurement

The HgTe QDs/PBDB-T:Y6 BPD was fabricated with an architecture of indium tin oxide (ITO) (cathode)/PBDB-T:Y6 (organic active layer)/ZnO (ETL)/HgTe QDs (active layer)/MoO_3 (HTL)/Ag (anode). The substrates with patterned ITO were scrubbed with detergent and then sonicated in deionized water, acetone and isopropanol subsequently. The cleaned substrates were dried with a nitrogen stream and treated by UV-Ozone for 20 min before use. The active layer materials (PBDB-T:Y6 = 1:1.2 by weight) was dissolved in 1,2-dichlorobenzene (o-DCB) at a concentration of 10 mg/mL. The solutions were magnetically stirred overnight at 50 °C under nitrogen atmosphere. Before spin-coating, the organic active layer solution and substrates were preheated on a hot plate at 100 °C. The organic solution was dropped onto an ITO substrate and spin coated at 4000 rpm for 40 s. The organic active layers were then thermally annealed at 110 °C for 10 min under nitrogen atmosphere. The ZnO layer (20 nm) was sequentially

thermally evaporated under 10^{-4} Pa. The HgTe QDs active layer was spin coated layer by layer on a ZnO substrate, with each layer consisting of 3 steps: (1) The solution of HgTe QDs (90 mg/mL) was dropped onto a ZnO substrate and spin coated at 2000 rpm for 20 s. (2) Then the film was covered with EDT/IPA (v/v=1:500) solution for 30 s and spin coated at 2000 rpm for 20 s. (3) Finally, the IPA was used to clean the residual EDT on the surface of the film, and excess IPA was removed by spin coating at 2000 rpm for 20 s, and the film was annealed at 50 °C for 10 min. This process was repeated 8–10 times to obtain a film with a thickness of 120 nm. Finally, the MoO_3 layer (10 nm) and Ag layer (100 nm) were sequentially thermally evaporated under 10^{-4} Pa. The I–V curves, photocurrent broadband response spectrum, D*, and R spectra were measured with a semiconductor characterization system (Keithley 4200) under a Xenon light source coupled with a monochromator, calibrated with a standard Si detector (S1337-1010BQ, Hamamatsu Photonics) and InGaAs detector (Hamamatsu Photonics). The response time were measured by a semiconductor parameter analyzer (PD-RS, Enli Technology). Specially, 400 and 1550 nm LED light are used for the implementation of optoelectronic logic gates.

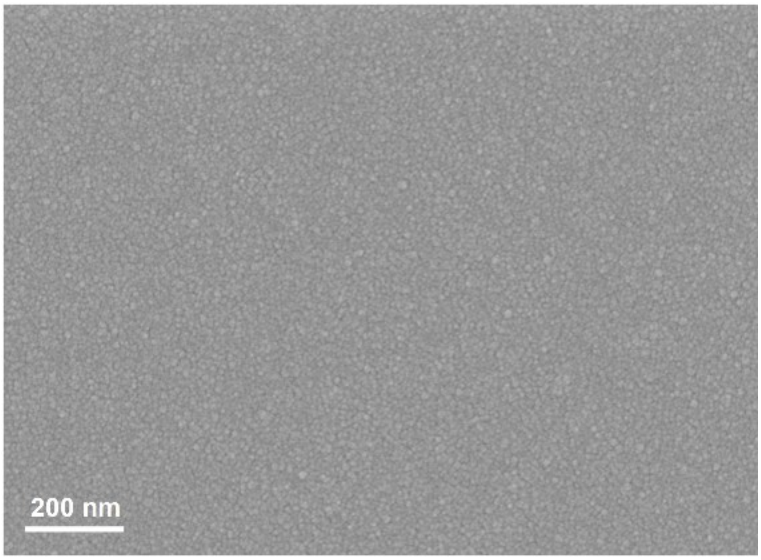

Fig. S1 SEM image of the PBDB-T:Y6 film.

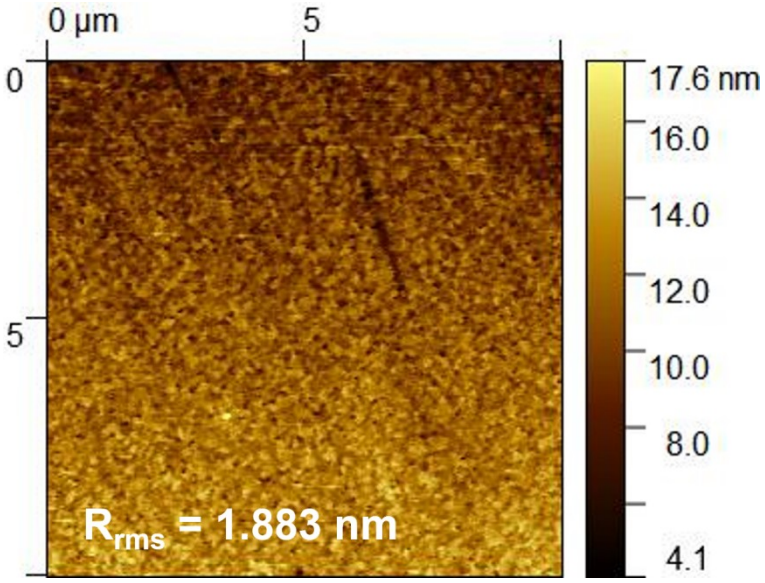

Fig. S2 AFM images of the PBDB-T:Y6 film.

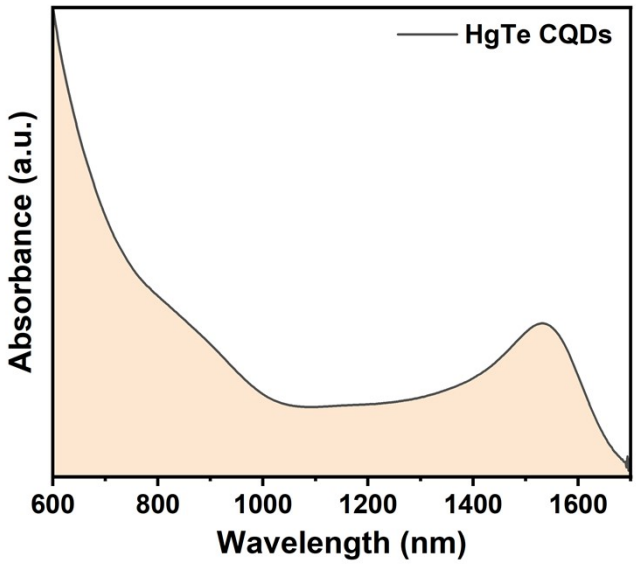

Fig. S3 Absorption spectra of the HgTe QDs solution.

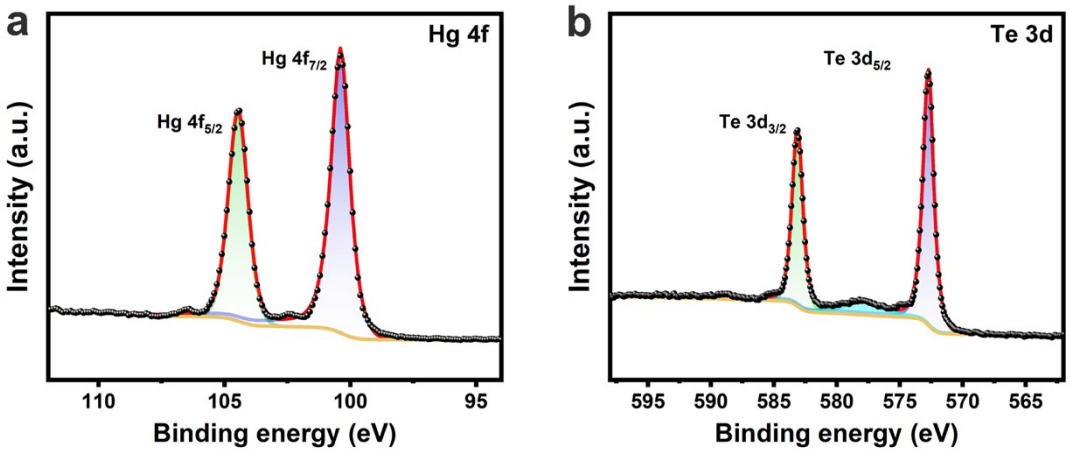

Fig. S4 (a)Hg 4f and (b) Te 3d spectra of the HgTe QDs film.

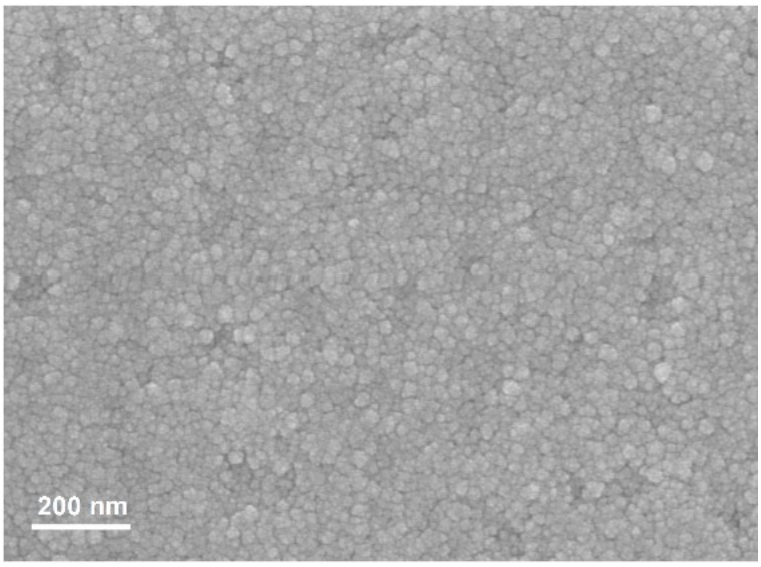

Fig. S5 SEM image of the HgTe QDs film.

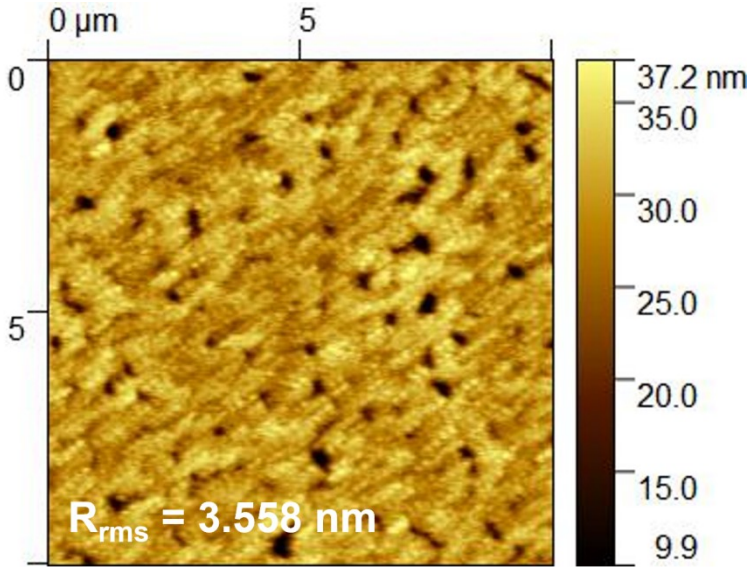

Fig. S6 AFM image of the HgTe QDs film.

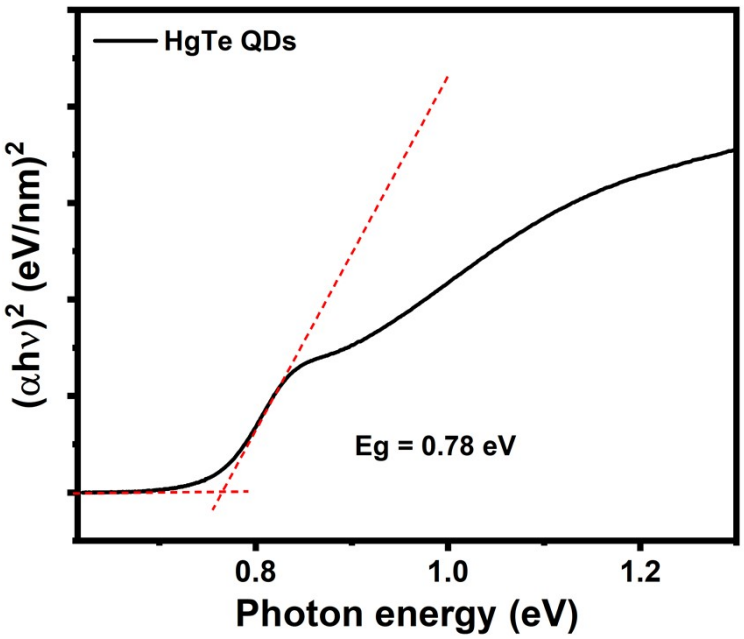

Fig. S7 Tauc plot of the HgTe QDs film.

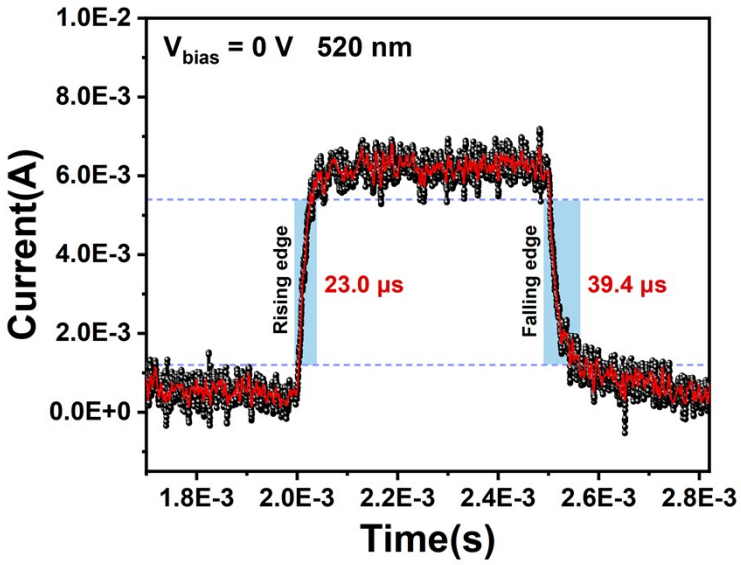

Fig. S8 Response and recovery times of the HgTe QDs/PBDB-T:Y6 BPD.

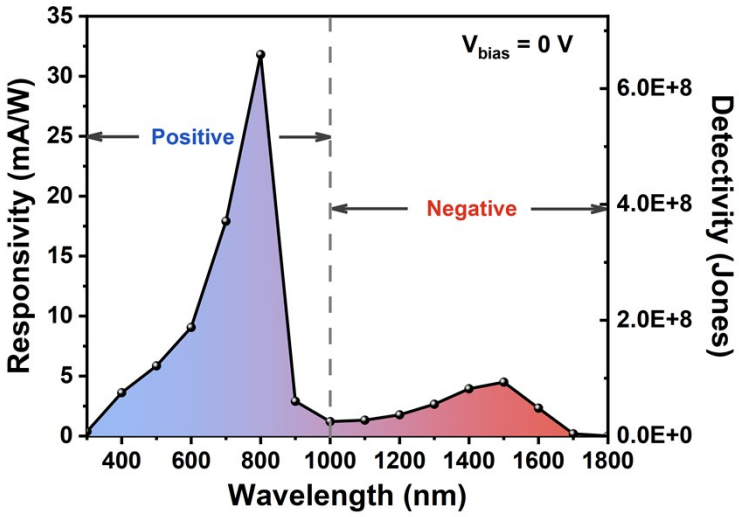

Fig. S9 Broadband responsivity and detectivity of the HgTe QDs/PBDB-T:Y6 BPD.

Table S1. Comparisons of the HgTe QDs/PBDB-T:Y6 BPD and other reported photodiode-type BPDs.

Materials	Maximum responsivity (mA/W)	Maximum detectivity (Jones)	Response range (nm)	Response/ recovery time	Ref.
CdTe/SnSe nanorods	2.1×10^{-2}	/	405–2000	20.9/39.6 ms	1
2D perovskite $FA_3Bi_2I_9$	/	/	300–1100	/	2
$MAPbCl_3$/$MAPbBr_3$/$MAPbI_3$ perovskites	32.47	7.82×10^{11}	300–900	0.16 s	3
$CH_3NH_3PbBr_3$/$PbZr_{0.52}Ti_{0.48}O_3$	0.22	/	300–600	43/7 ms	4
SnS_x nanoflakes/TiO_2 nanorod arrays	12.75	1.43×10^{11}	385–410	/	5
ITO/ $BaTiO_3$/Ag	9.85×10^{-2}	1.25×10^{10}	365–760	83/47 ms	6
p-NiO/n-ZnO/p-Si	625	5.52×10^{10}	325–785	1.7/1.6 ms	7
ZnO nanowires/Sb_2Se_3	4.08×10^{-2}	/	405–880	43/44 ms	8
PTB7-Th:$PC_{71}BM$/PTB7-Th:CO_i 8DFIC:$PC_{71}BM$	435	2×10^{12}	350–1100	17.5 ms	9
Sb_2Se_3/ZnO	77.66	2.45×10^{11}	365–1064	39/118 μs	10
ZnO/Cu_2O	550	1.5×10^{13}	365–470	2 ms	11
$FA_{0.5}MA_{0.5}Pb_{0.4}Sn_{0.6}I_3$/$MAPbI_3$	8.7	1.89×10^{11}	400–1000	40/72 μs	12
$FA0_{.992}MA_{0.008}Pb(I_{0.992}Br_{0.008})_3$/PM6/BTP-eC9/BTP-2F2Cl-P2EH	/	1.34×10^{12}	300–1000	9.02/11.42 μs	13
ZnO nanowires/SnS	3.64×10^{-2}	/	365–880	0.4/0.2 s	14
ITO/Cu/Au/N2200/Cu-doped $FAPbI_3$/n-Si	330	/	300–1100	139/2.8 μs	15
$BaTiO_3$/$LaNiO_3$	/		360–980	103/540 μs	16
HgTe QDs/PBDB-T:Y6	32.6	8.7×10^{8}	300–1800	23.0/39.4 μs	This work

Supplementary References

1. G. C. Liu, F. H. Guo, M.C. Zhang, Y. J. Liu, J. Y. Hao, W. Z. Yu, S. Q. Li, B. Hu, B. Zhang and L. Z. Hao, *ACS Appl. Mater. Interfaces*, 2023, **15**, 29375–29383.
2. W. J. Cheng, S. L. Wu, J. Y. Lu, G. Y. Li, S. H. Li, W. Tian and L. Li, *Adv. Mater.*, 2024, **36**, 2307534.
3. Y. Li, F. M. Guo, S. S. Yu, J. Wang and S. H. Yang, *Nano Futures*, 2022, **6**, 025006.
4. X. M. Shen, S. Y. Chen, Y. H. Liu, M. M. Chen, H. Lei, J. Cai, J. Y. Su, S. H. Yang, Y. Liu, Q. Wang, D. W. Cao and C. X. Xu, *Appl. Phys. Lett.*,2022, **120**, 091107.
5. J. Chen, J. P. Xu, L. N. Kong, S. B. Shi, J. H. Xu, S. Y. Gao, X. S. Zhang and L. Li, *J. Colloid Interface Sci.*, 2024, **663**, 336–344.
6. C. X. Li, C. Chen, L. Zhao and N. Ma, *ACS Appl. Mater. Interfaces*, 2023, **15**, 23402–23411.
7. Y. L. Zhang, H. Y. Xue, M. Zhu and Z. N. Wang, *J. Appl. Phys.*, 2023, **134**, 094502.
8. B. S. Ouyang, H. Q. Zhao, Z. L. Wang and Y. Yang, *Nano Energy*, 2020, **68**, 104312.
9. Z. J. Lan, Y. S. Lau, L. F. Cai, J. Y. Han, C. W. Suen and F. R. Zhu, *Laser Photonics Rev.*, 2022, **16**, 2100602.
10. J. C. Jiang, Y. J. Guo, X. L. Weng, F. C. Long, Y. Xin, Y. F. Lu, Z. Z. Ye, S. C. Ruan and Y. -J. Zeng, *J. Mater. Chem. C*, 2021, **9**, 4978–4988.
11. Y. C. Bu, J. P. Xu, K. Li, S. B. Shi, J. Chen, M. H. Li, Q. Y. Zhang, P. C. Yang, J. H. Xu, X. S. Zhang, L. N. Kong and L. Li, *J. Mater. Chem. C*, 2021, **9**, 6885–6893.
12. W. Kim, H. Kim, T. J. Yoo, J. Y. Lee, J. Y. Jo, B. H. Lee, A. A. Sasikala, G. Y. Jung and Y. Pak, *Nat. Commun.*, 2022, **13**, 720.

13. D. Zhao, Y. Wang, X. L. Sun, X. Wu, B. Li, S. F. Zhang, D. P. Gao, B. Z. Liu, S. K. Gong, Z. Li, C. L. Zhang, X. H. Chen, S. Xiao, S. F. Yang, Z. Li and Z. L. Zhu, *Small*, 2024, **20**, 2309827.
14. B. S. Ouyang, K. W. Zhang and Y. Yang, *iScience*, 2018, **1**, 16–23.
15. L. K. Bian, F. R. Cao, H. Zhao, F. Xiang, H. X. Sun, M. Wang and L. Li, *Laser Photonics Rev.*, 2024, https://doi.org/10.1002/lpor.202401331.
16. H. Y. Dan, H. Y. Li, L. Xu, C. Guo, C. R. Bowen and Y. Yang, *InfoMat.*, 2024, **6**, e12531.